2.3 Mirrors, Interferometers and Thin-Film Structures

One of the most striking wave phenomena is interference. Many optical devices are based on the concept of interfering waves, such as low loss dielectric mirrors and interferometers and other thin-film optical coatings. After having a quick look into the phenomenon of interference, we will develope a powerful matrix formalism that enables us to evaluate efficiently many optical (also microwave) systems based on interference.

2.3.1 Interference and Coherence

Interference

Interference of waves is a consequence of the linearity of the wave equation (2.13). If we have two individual solutions of the wave equation

$$\vec{E}_1(\vec{r},t) = E_1 \cos(\omega_1 t - \vec{k}_1 \cdot \vec{r} + \varphi_1)\ \vec{e}_1, \tag{2.137}$$

$$\vec{E}_2(\vec{r},t) = E_2 \cos(\omega_2 t - \vec{k}_1 \cdot \vec{r} + \varphi_2)\ \vec{e}_2, \tag{2.138}$$

with arbitrary amplitudes, wave vectors and polarizations, the sum of the two fields (superposition) is again a solution of the wave equation

$$\vec{E}(\vec{r},t) = \vec{E}_1(\vec{r},t) + \vec{E}_2(\vec{r},t). \tag{2.139}$$

If we look at the intensity, wich is proportional to the amplitude square of the total field

$$\vec{E}(\vec{r},t)^2 = \left(\vec{E}_1(\vec{r},t) + \vec{E}_2(\vec{r},t)\right)^2, \tag{2.140}$$

we find

$$\vec{E}(\vec{r},t)^2 = \vec{E}_1(\vec{r},t)^2 + \vec{E}_2(\vec{r},t)^2 + 2\vec{E}_1(\vec{r},t)\cdot\vec{E}_2(\vec{r},t) \tag{2.141}$$

with

$$\vec{E}_1(\vec{r},t)^2 = \frac{E_1^2}{2}\left(1+\cos 2(\omega_1 t - \vec{k}_1\cdot\vec{r}+\varphi_1)\right), \tag{2.142}$$

$$\vec{E}_2(\vec{r},t)^2 = \frac{E_2^2}{2}\left(1+\cos 2(\omega_2 t - \vec{k}_2\cdot\vec{r}+\varphi_2)\right), \tag{2.143}$$

$$\begin{aligned}\vec{E}_1(\vec{r},t)\cdot\vec{E}_2(\vec{r},t) &= (\vec{e}_1\cdot\vec{e}_2)\,E_1E_2\cos(\omega_1 t - \vec{k}_1\cdot\vec{r}+\varphi_1)\cdot \\ &\quad\cdot\cos(\omega_2 t - \vec{k}_2\cdot\vec{r}+\varphi_2)\end{aligned} \tag{2.144}$$

$$\vec{E}_1(\vec{r},t)\cdot\vec{E}_2(\vec{r},t) = \frac{1}{2}(\vec{e}_1\cdot\vec{e}_2)\,E_1E_2\cdot \tag{2.145}$$

$$\cdot\left[\begin{array}{l}\cos\left((\omega_1-\omega_2)\,t-\left(\vec{k}_1-\vec{k}_2\right)\cdot\vec{r}+(\varphi_1-\varphi_2)\right) \\ +\cos\left((\omega_1+\omega_2)\,t-\left(\vec{k}_1+\vec{k}_2\right)\cdot\vec{r}+(\varphi_1+\varphi_2)\right)\end{array}\right] \tag{2.146}$$

Since at optical frequencies neither our eyes nor photo detectors, can ever follow the optical frequency itself and certainly not twice as large frequencies, we drop the rapidly oscillating terms. Or in other words we look only on the cycle-averaged intensity, which we denote by a bar

$$\begin{aligned}\overline{\vec{E}(\vec{r},t)^2} &= \frac{E_1^2}{2}+\frac{E_2^2}{2}+(\vec{e}_1\cdot\vec{e}_2)\,E_1E_2\cdot \\ &\quad\cdot\cos\left((\omega_1-\omega_2)\,t-\left(\vec{k}_1-\vec{k}_2\right)\cdot\vec{r}+(\varphi_1-\varphi_2)\right)\end{aligned} \tag{2.147}$$

Depending on the frequencies ω_1 and ω_2 and the deterministic and stochastic properties of the phases φ_1 and φ_2, we can detect this periodically varying intensity pattern called interference pattern. Interference of waves can be best visuallized with water waves, see Figure 2.38. Note, however, that water waves are a scalar field, whereas the EM-waves are vector waves. Therefore, the interference phenomena of EM-waves are much richer in nature than

for water waves. Notice, from Eq.(2.147), it follows immedicatly that the interference vanishes in the case of orthogonally polarized EM-waves, because of the scalar product involved. Also, if the frequencies of the waves are not identical, the interference pattern will not be stationary in time.

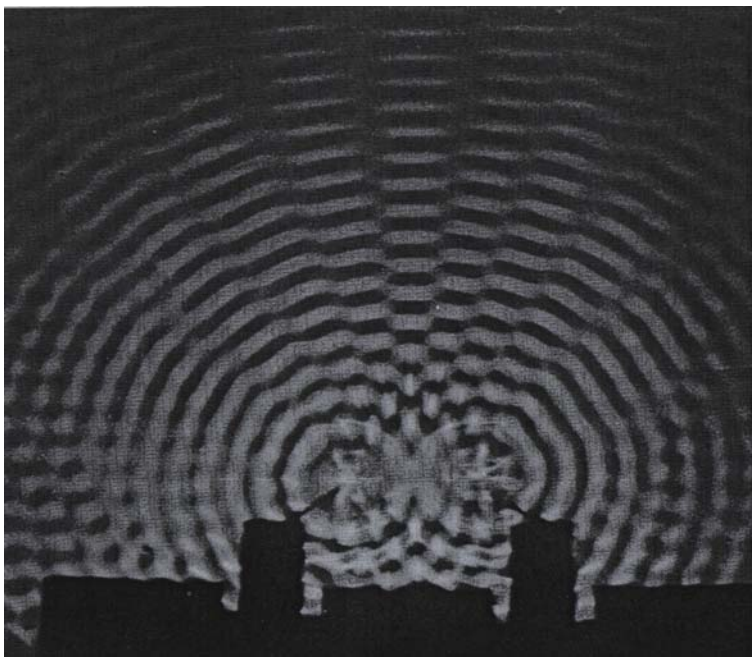

Figure 2.38: Interference of water waves from two point sources in a ripple tank [1] p. 276.

If the frequencies are identical, the interference pattern depends on the wave vectors, see Figure 2.39. The interference pattern which has itself a wavevector given by

$$\vec{k}_1 - \vec{k}_2 \tag{2.148}$$

shows a period of

$$\Lambda = \frac{2\pi}{\left|\vec{k}_1 - \vec{k}_2\right|}. \tag{2.149}$$

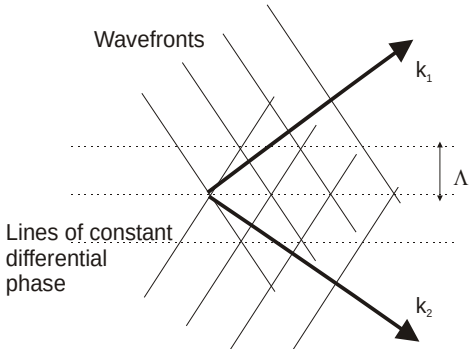

Figure 2.39: Interference pattern generated by two monochromatic plane waves.

Coherence

The ability of waves to generate an interference pattern is called coherence. Coherence can be quantified both temporally or spatially. For example, if we are at a certain position $\vec{r}$ in the interference pattern described by Eq.(2.147), we will only have stationary conditions over a time interval

$$T_{coh} << \frac{2\pi}{\omega_1 - \omega_2}.$$

Thus the spectral width of the waves determines the temporal coherence. However, it depends very often on the expermental arrangement whether a given situation can still lead to interference or not. Even so the interfering light may be perfectly temporally coherent, i.e. perfectly monochromatic, $\omega_1 = \omega_2$,yet the wave vectors may not be stable over time and the spatial inteference pattern may wash out, i.e. there is insufficient spatial coherence. So for stable and maximum interference three conditions must be fulfilled:

- stable and identical polarization
- small change in the relative phase between the beams involved over the observation time, temporal coherence, often achieved by using narrrow linewidth light
- stable beam propagation or guiding of light to achieve spatial coherence.

It is by no means trivial to arrive at a light source and an experimental setup that enables good coherence and strong interference of the beams involved.

Interference of beams can be used to measure relative phase shifts between them which may be proportional to a physical quantity that needs to be measured. Such phase shifts between two beams can also be used to modulate the light output at a given position in space via interference. In 6.013, we have already encountered interference effects between forward and backward traveling waves on transmission lines. This is very closely related to what we use in optics, therefore, we quickly relate the TEM-wave progagation to the transmission line formalism developed in Chapter 5 of 6.013.

2.3.2 TEM-Waves and TEM-Transmission Lines

The motion of voltage V and current I along a TEM transmission line with an inductance L' and a capacitance $C\prime$ per unit length is satisfies

$$\frac{\partial V(t,z)}{\partial z} = -L'\frac{\partial I(t,z)}{\partial t} \tag{2.150}$$

$$\frac{\partial I(t,z)}{\partial z} = -C'\frac{\partial V(t,z)}{\partial t} \tag{2.151}$$

Substitution of these equations into each other results in wave equations for either the voltage or the current

$$\frac{\partial^2 V(t,z)}{\partial z^2} - \frac{1}{c^2}\frac{\partial^2 V(t,z)}{\partial t^2} = 0, \tag{2.152}$$

$$\frac{\partial^2 I(t,z)}{\partial z^2} - \frac{1}{c^2}\frac{\partial^2 I(t,z)}{\partial t^2} = 0, \tag{2.153}$$

where $c = 1/\sqrt{L'C'}$ is the speed of wave propagation on the transmission line. The ratio between voltage and current for monochomatic waves is the characteristic impedance $Z = \sqrt{L'/C'}$.

The equations of motion for the electric and magnetic field of a x-polarized TEM wave according to Figure 2.1, with $E-$field along the x-axis and H-fields along the y- axis follow directly from Faraday's and Ampere's law

$$\frac{\partial E(t,z)}{\partial z} = -\mu\frac{\partial H(t,z)}{\partial t}, \tag{2.154}$$

$$\frac{\partial H(t,z)}{\partial z} = -\varepsilon\frac{\partial E(t,z)}{\partial t}, \tag{2.155}$$

which are identical to the transmission line equations (2.150) and (2.151). Substitution of these equations into each other results again in wave equations for electric and magnetic fields propagating at the speed of light $c = 1/\sqrt{\mu\varepsilon}$ and with characteristic impedance $Z_F = \sqrt{\mu/\varepsilon}$.

The solutions of the wave equation are forward and backward traveling waves, which can be decoupled by transforming the fields to the forward and backward traveling waves

$$a(t,z) = \sqrt{\frac{A_{eff}}{2Z_F}}\left(E(t,z) + Z_{Fo}H(t,z)\right), \tag{2.156}$$

$$b(t,z) = \sqrt{\frac{A_{eff}}{2Z_F}}\left(E(t,z) - Z_{Fo}H(t,z)\right), \tag{2.157}$$

which fulfill the equations

$$\left(\frac{\partial}{\partial z} + \frac{1}{c}\frac{\partial}{\partial t}\right)a(t,z) = 0, \tag{2.158}$$

$$\left(\frac{\partial}{\partial z} - \frac{1}{c}\frac{\partial}{\partial t}\right)b(t,z) = 0. \tag{2.159}$$

Note, we introduced that cross section A_{eff} such that $|a|^2$ is proportional to the total power carried by the wave. Clearly, the solutions are

$$a(t,z) = f(t - z/c_0), \tag{2.160}$$

$$b(t,z) = g(t + z/c_0), \tag{2.161}$$

which resembles the D'Alembert solutions of the wave equations for the electric and magnetic field

$$E(t,z) = \sqrt{\frac{Z_{Fo}}{2A_{eff}}}\left(a(t,z) + b(t,z)\right), \tag{2.162}$$

$$H(t,z) = \sqrt{\frac{1}{2Z_{Fo}A_{eff}}}\left(a(t,z) - b(t,z)\right). \tag{2.163}$$

Here, the forward and backward propagating fields are already normalized such that the Poynting vector multiplied with the effective area gives already the total power transported by the fields in the effective cross section A_{eff}

$$P = \vec{S}\cdot\left(A_{eff}\ \vec{e}_z\right) = A_{eff}E(t,z)H(t,z) = |a(t,z)|^2 - |b(t,z)|^2. \tag{2.164}$$

In 6.013, it was shown that the relation between sinusoidal current and voltage waves

$$V(t,z) = \mathrm{Re}\left\{\underline{V}(z)e^{j\omega t}\right\} \text{ and } I(t,z) = \mathrm{Re}\left\{\underline{I}(z)e^{j\omega t}\right\} \tag{2.165}$$

along the transmission line or corresponding electric and magnetic fields in one dimensional wave propagation is described by a generalized complex impedance $\underline{Z}(z)$ that obey's certain transformation rules, see Figure 2.40 (a).

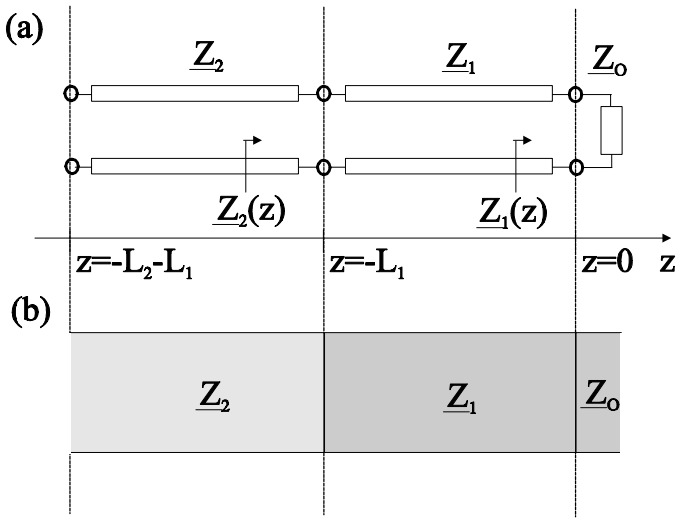

Figure 2.40: (a) Transformation of generalized impedance along transmission lines, (b) Transformation of generalized impedance accross free space sections with different characterisitc wave impedances in each section.

Along the first transmission line, which is terminated by a load impedance, the generalized impedance transforms according to

$$\underline{Z}_1(z) = \underline{Z}_1 \cdot \frac{\underline{Z}_0 - j\underline{Z}_1 \tan(k_1 z)}{\underline{Z}_1 - j\underline{Z}_0 \tan(k_1 z)} \tag{2.166}$$

with $k_1 = k_0\underline{n}_1$ and along the second transmission line the same rule applies as an example

$$\underline{Z}_2(z) = \underline{Z}_2 \cdot \frac{\underline{Z}_1(-L_1) - j\underline{Z}_2 \tan(k_2 z)}{\underline{Z}_2 - j\underline{Z}_1(-L_1) \tan(k_2 z)} \tag{2.167}$$

with $k_2 = k_0 n_2$. Note, that the media can also be lossy, then the characteristic impedances of the transmission lines and the propagation constants are already themselves complex numbers. The same formalism can be used to solve corresponding one dimensional EM-wave propagation problems.

Antireflection Coating

The task of an antireflection (AR-)coating, analogous to load matching in transmission line theory, is to avoid reflections between the interface of two media with different optical properties. One method of course could be to place the interface at Brewster's angle. However, this is not always possible. Let's assume we want to put a medium with index n into a beam under normal incidence, without having reflections on the air/medium interface. The medium can be for example a lens. This is exactly the situation shown in Figure 2.40 (b). $\underline{Z}_2$ describes the refractive index of the lense material, e.g. $n_2 = 3.5$ for a silicon lense, we can deposit on the lens a thin layer of material with index n_1 corresponding to $\underline{Z}_1$ and this layer should match to the free space index $n_0 = 1$ or impedance $\underline{Z}_0 = 377\Omega$. Using (2.166) we obtain

$$\underline{Z}_2 = \underline{Z}_1(-L_1) = \underline{Z}_1 \frac{\underline{Z}_0 - j\underline{Z}_1 \tan(-k_1 L_1)}{\underline{Z}_1 - j\underline{Z}_0 \tan(-k_1 L_1)} \tag{2.168}$$

If we choose a quarter wave thick matching layer $k_1 L_1 = \pi/2$, this simplifies to the famous result

$$\underline{Z}_2 = \frac{\underline{Z}_1^2}{\underline{Z}_0}, \tag{2.169}$$

$$\text{or } n_1 = \sqrt{n_2 n_0} \text{ and } L_1 = \frac{\lambda}{4 n_1}. \tag{2.170}$$

Thus a quarter wave AR-coating needs a material which has an index corresponding to the geometric mean of the two media to be matched. In the current example this would be $n_2 = \sqrt{3.5} \approx 1.87$

2.3.3 Scattering and Transfer Matrix

Another formalism to analyze optical systems (or microwave circuits) can be formulated using the forward and backward propagating waves, which transform much simpler along a homogenous transmission line than the total fields, i.e. the sum of forward adn backward waves. However, at interfaces

scattering of these waves occurs whereas the total fields are continuous. For monochromatic forward and backward propagating waves

$$\underline{a}(t,z) = \underline{a}(z)e^{j\omega t} \text{ and } \underline{b}(t,z) = \underline{b}(z)e^{j\omega t} \tag{2.171}$$

propagating in z-direction over a distance z with a propagation constant k, we find from Eqs.(2.158) and (2.159)

$$\begin{pmatrix} \underline{a}(z) \\ \underline{b}(z) \end{pmatrix} = \begin{pmatrix} e^{-jkz} & 0 \\ 0 & e^{jkz} \end{pmatrix} \begin{pmatrix} \underline{a}(0) \\ \underline{b}(0) \end{pmatrix}. \tag{2.172}$$

A piece of transmission line is a two port. The matrix transforming the amplitudes of the waves at the input port (1) to those of the output port (2) is called the transfer matrix, see Figure 2.41

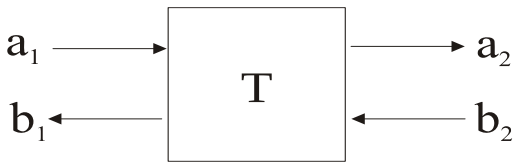

Figure 2.41: Definition of the wave amplitudes for the transfer matrix T.

For example, from Eq.(2.172) follows that the transfer matrix for free space propagation is

$$\mathbf{T} = \begin{pmatrix} e^{-jkz} & 0 \\ 0 & e^{jkz} \end{pmatrix}. \tag{2.173}$$

This formalism can be expanded to arbitrary multiports. Because of its mathematical properties the scattering matrix that describes the transformation between the incoming and outgoing wave amplitudes of a multiport is often used, see Figure 2.42.

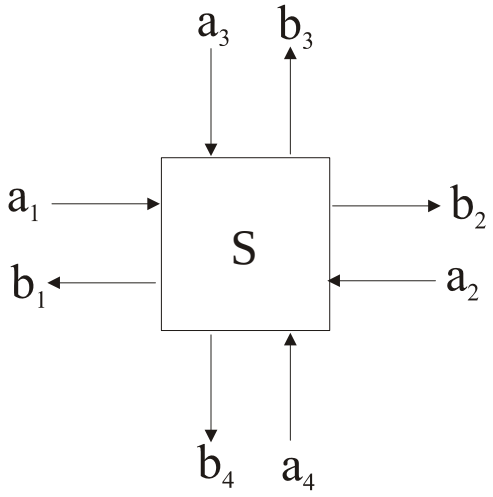

Figure 2.42: Scattering matrix and its port definition.

The scattering matrix defines a linear transformation from the incoming to the outgoing waves

$$\vec{\underline{b}} = \underline{\mathbf{S}}\vec{\underline{a}}, \text{ with } \underline{a} = (a_1, a_2, ...)^T \,, \; \underline{b} = (b_1, b_2, ...)^T \,. \tag{2.174}$$

Note, that the meaning between forward and backward waves no longer coincides with $\underline{a}$ and $\underline{b}$, a connection, which is difficult to maintain if several ports come in from many different directions.

The transfer matrix T has advantages, if many two ports are connected in series with each other. Then the total transfer matrix is the product of the individual transfer matrices.

2.3.4 Properties of the Scattering Matrix

Physial properties of the system reflect itself in the mathematical properties of the scattering matrix.

Reciprocity

A system with constant scalar dielectric and magnetic properties must have a symmetric scattering matrix (without proof)

$$\underline{\mathbf{S}} = \underline{\mathbf{S}}^T. \tag{2.175}$$

Losslessness

In a lossless system the total power flowing into the system must be equal to the power flowing out of the system in steady state

$$|\vec{\underline{a}}|^2 = \left|\vec{\underline{b}}\right|^2, \tag{2.176}$$

i.e.

$$\underline{\mathbf{S}}^+\underline{\mathbf{S}} = 1 \text{ or } \underline{\mathbf{S}}^{-1}=\underline{\mathbf{S}}^+. \tag{2.177}$$

The scattering matrix of a lossless system must be unitary.

Time Reversal

To find the scattering matrix of the time reversed system, we realize that incoming waves become outgoing waves under time reversal and the other way around, i.e. the meaning of $\underline{a}$ and $\underline{b}$ is exchanged and on top of it the waves become negative frequency waves.

$$\underline{a}e^{j(\omega t-kz)} \overset{\text{time reversal}}{\rightarrow} \underline{a}e^{j(-\omega t-kz)}. \tag{2.178}$$

To obtain the complex amplitude of the corresponding positive frequency wave, we need to take the complex conjugate value. So to obtain the equations for the time reversed system we have to perform the following substitutions

$$\begin{array}{cc} \text{Original system} & \text{Time reversed system} \\ \vec{\underline{b}} = \underline{\mathbf{S}}\vec{\underline{a}} & \vec{\underline{a}}^* = \underline{\mathbf{S}}\vec{\underline{b}}^* \rightarrow \vec{\underline{b}} = \left(\underline{\mathbf{S}}^{-1}\right)^* \vec{\underline{a}} \end{array}. \tag{2.179}$$

2.3.5 Beamsplitter

As an example, we look at the scattering matrix for a partially transmitting mirror, which could be simply formed by the interface between two media with different refractive index, which we analyzed in the previous section, see Figure 2.43. (Note, for brevity we neglect the reflections at the normal surface input to the media, or we put an AR-coating on them.) In principle, this device has four ports and should be described by a 4x4 matrix. However, most often only one of the waves is used at each port, as shown in Figure 2.43.

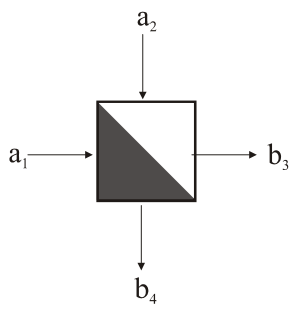

Figure 2.43: Port definitions for the beam splitter

The scattering matrix is determined by

$$\vec{\underline{b}} = \underline{\mathbf{S}}\vec{\underline{a}}, \text{ with } \underline{a} = (a_{1,}a_2)^T \ , \ \vec{\underline{b}} = (b_3, b_4)^T \tag{2.180}$$

and

$$\mathbf{S}= \begin{pmatrix} r & jt \\ jt & r \end{pmatrix}, \text{ with } r^2 + t^2 = 1. \tag{2.181}$$

The matrix $\mathbf{S}$ was obtained using using the S-matrix properties described above. From Eqs.(2.113) we could immediately identify r as a function of the refractive indices, angle of incidence and the polarization used. Note, that the off-diagonal elements of $\mathbf{S}$ are identical, which is a consequence of reciprocity. That the main diagonal elements are identical is a consequence of unitarity for a lossless beamsplitter and furthermore $t = \sqrt{1 - r^2}$. For a given frequency r and t can always be made real by choosing proper reference planes at the input and the output of the beam splitter. Beamsplitters can be made in many ways, see for example Figure 2.37.

2.3.6 Interferometers

Having a valid description of a beamsplitter at hand, we can build and analyze various types of interferometers, see Figure 2.44.

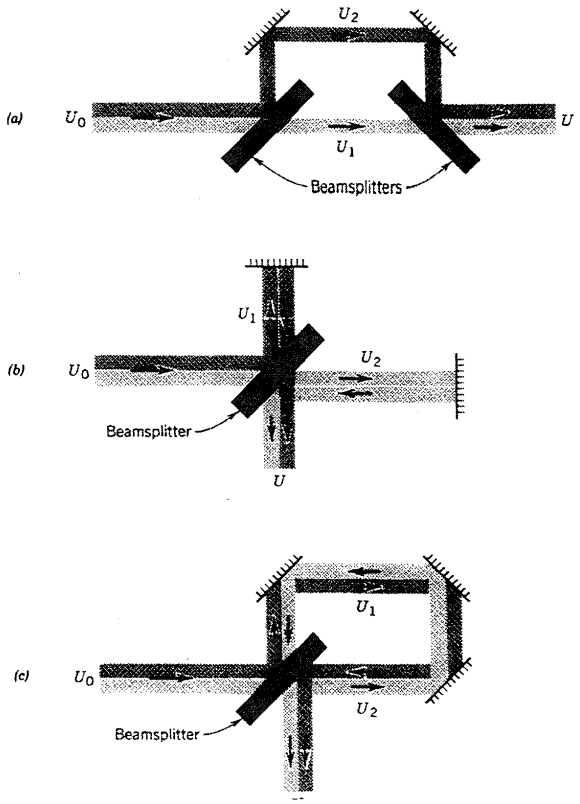

Figure 2.44: Different types of interferometers: (a) Mach-Zehnder Interferometer; (b) Michelson Interferometer; (c) Sagnac Interferometer [6] p. 66.

Each of these structures has advantages and disadvantages depending on the technology they are realized. The interferometer in Figure 2.44 (a) is called Mach-Zehnder interferometer, the one in Figure 2.44 (b) is called Michelson Interferometer. In the Sagnac interferometer , Figure 2.44 (c) both beams see identical beam path and therefore errors in the beam path can be balance out and only differential changes due to external influences lead to an output signal, for example rotation, see problem set 3.

To understand the light transmission through an interferometer we analyze as an example the Mach-Zehnder interferometer shown in Figure 2.45. If we excite input port 1 with a wave with complex amplitude $\underline{a}_0$ and no input at port 2 and assume 50/50 beamsplitters, the first beam splitter will

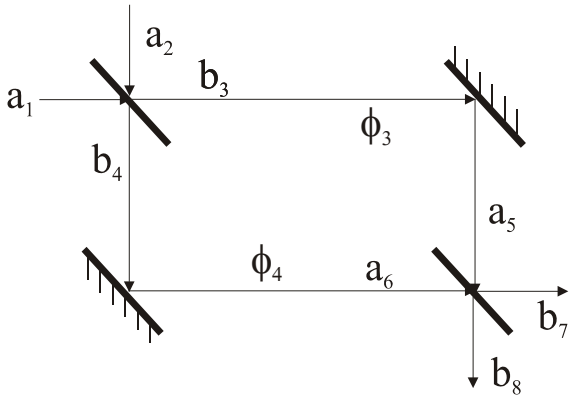

Figure 2.45: Mach-Zehnder Interferometer

produce two waves with complex amplitudes

$$\begin{aligned} \underline{b}_3 &= \tfrac{1}{\sqrt{2}}\underline{a}_0 \\ \underline{b}_4 &= j\tfrac{1}{\sqrt{2}}\underline{a}_0 \end{aligned} \tag{2.182}$$

During propagation through the interferometer arms, both waves pick up a phase delay $\phi_3 = kL_3$ and $\phi_4 = kL_4$, respectively

$$\begin{aligned} a_5 &= \tfrac{1}{\sqrt{2}}\underline{a}_0 e^{-j\phi_3}, \\ a_6 &= j\tfrac{1}{\sqrt{2}}\underline{a}_0 e^{-j\phi_4}. \end{aligned} \tag{2.183}$$

After the second beam splitter with the same scattering matrix as the first one, we obtain

$$\begin{aligned} b_7 &= \tfrac{1}{2}\underline{a}_0 \left(e^{-j\phi_3} - e^{-j\phi_4}\right), \\ b_8 &= j\tfrac{1}{2}\underline{a}_0 \left(e^{-j\phi_3} + e^{-j\phi_4}\right). \end{aligned} \tag{2.184}$$

The transmitted power to the output ports is

$$\begin{aligned} |b_7|^2 &= \tfrac{|\underline{a}_0|^2}{4}\left|1 - e^{-j(\phi_3-\phi_4)}\right|^2 = \tfrac{|\underline{a}_0|^2}{2}\left[1 - \cos\left(\phi_3 - \phi_4\right)\right], \\ |b_8|^2 &= \tfrac{|\underline{a}_0|^2}{4}\left|1 + e^{-j(\phi_3-\phi_4)}\right|^2 = \tfrac{|\underline{a}_0|^2}{2}\left[1 + \cos\left(\phi_3 - \phi_4\right)\right]. \end{aligned} \tag{2.185}$$

The total output power is equal to the input power, as it must be for a lossless system. However, depending on the phase difference $\Delta\phi = \phi_3 - \phi_4$ between both arms, the power is split differently between the two output ports, see Figure 2.46.With proper biasing, i.e. $\phi_3 - \phi_4 = \pi/2 + \Delta\phi$, the difference in

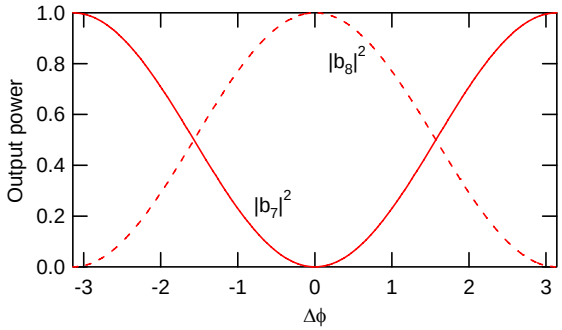

Figure 2.46: Output power from the two arms of an interfereometer as a function of phase difference.

output power between the two arms can be made directly proportional to the phase difference $\Delta\phi$.

Opening up the beam size in the interferometer and placing optics into the beam enables to visualize beam distortions due to imperfect optical components, see Figures 2.47 and 2.48.

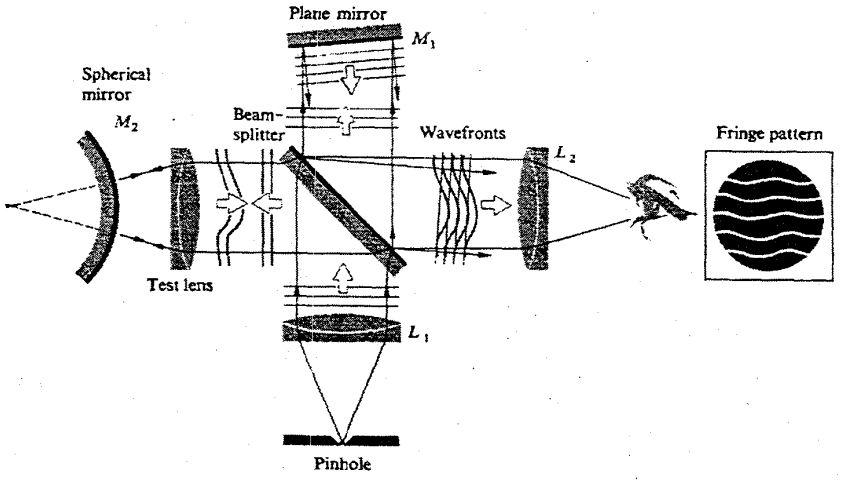

Figure 2.47: Twyman-Green Interferometer to test optics quality [1] p. 324.

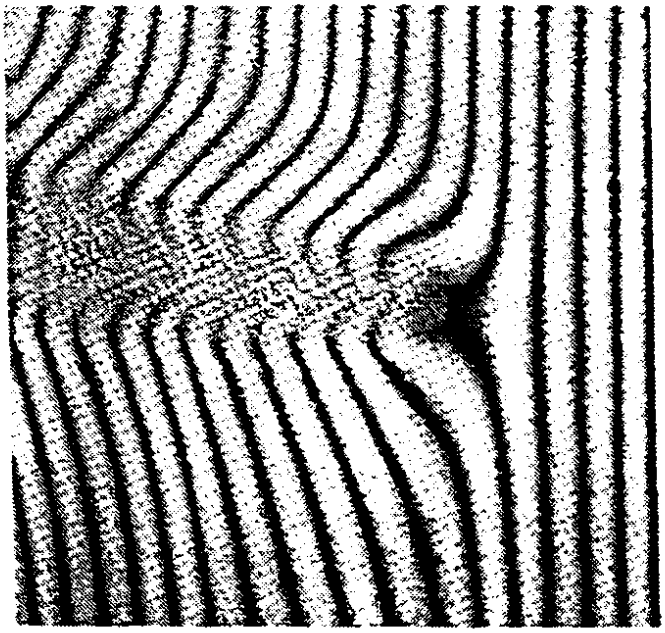

Figure 2.48: Interference pattern with a hot iron placed in one arm of the interferometer ([1], p. 395).

2.3.7 Fabry-Perot Resonator

Interferometers can act as filters. The phase difference between the interferometer arms depends on frequency, therefore, the transmission from input to output depends on frequency, see Figure 2.46. However, the filter function is not very sharp. The reason for this is that only a two beam interference is used. Much more narrowband filters can be constructed by multipass interferences such as in a Fabry-Perot Resonator, see Figure 2.49. The simplest Fabry Perot is described by a sequence of three layers where at least the middle layer has an index different from the other two layers, such that reflections occur on these interfaces.

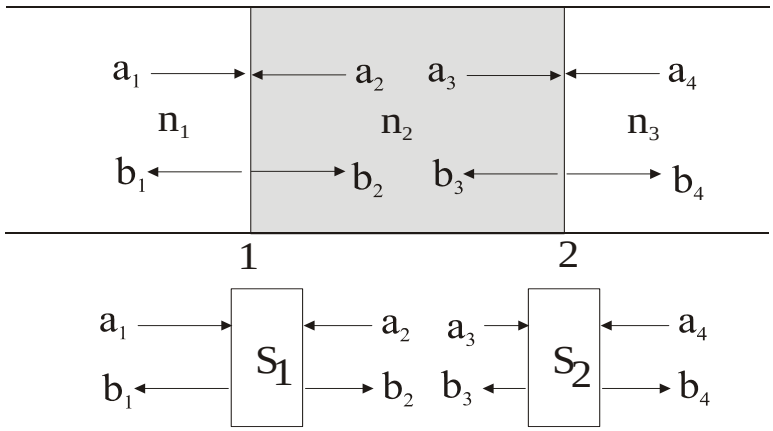

Figure 2.49: Multiple intereferences in a Fabry Perot resonator. In the simplest implementation a Fabry Perot only consists of a sequence of three layers with different refractive index so that two reflections occur with multiple interferences. Each of this discontinuites can be described by a scattering matrix.

Any kind of device that has reflections at two parallel interfaces may act as a Fabry Perot such as two semitransparent mirrors. A thin layer of material against air can act as a Fabry-Perot and is often called etalon. Given the reflection and transmission coefficients at the interfaces 1 and 2, we can write down the scattering matrices for both interfaces according to Eqs.(2.180) and (2.181).

$$\begin{pmatrix} \tilde{\underline{b}}_1 \\ \tilde{\underline{b}}_2 \end{pmatrix} = \begin{pmatrix} r_1 & jt_1 \\ jt_1 & r_1 \end{pmatrix} \begin{pmatrix} \tilde{\underline{a}}_1 \\ \tilde{\underline{a}}_2 \end{pmatrix} \text{ and } \begin{pmatrix} \tilde{\underline{b}}_3 \\ \tilde{\underline{b}}_4 \end{pmatrix} = \begin{pmatrix} r_2 & jt_2 \\ jt_2 & r_2 \end{pmatrix} \begin{pmatrix} \tilde{\underline{a}}_3 \\ \tilde{\underline{a}}_4 \end{pmatrix}. \tag{2.186}$$

If we excite the Fabry-Perot with a wave from the right with amplitude. $\tilde{\underline{a}}_1 \neq 0$, then a fraction of that wave will be transmitted to the interface into the Fabry-Perot as wave $\tilde{\underline{b}}_2$ and part will be already reflected into $\tilde{\underline{b}}_1$,

$$\tilde{\underline{b}}_1^{(0)} = r_1 \tilde{\underline{a}}_1. \tag{2.187}$$

The transmitted wave will then propagate and pick up a phase factor $e^{-j\phi/2}$, with $\phi = 2k_2 L$ and $k_2 = \frac{2\pi}{\lambda} n_2$,

$$\tilde{\underline{a}}_3 = \mathrm{j}t\tilde{\underline{a}}_1 e^{-j\phi/2}. \tag{2.188}$$

After propagation it will be reflected off from the second interface which has a reflection coefficient

$$\Gamma_2 = \left.\frac{\tilde{\underline{b}}_3}{\tilde{\underline{a}}_3}\right|_{\underline{a}_4=0} = r_2. \tag{2.189}$$

Then the reflected wave $\tilde{\underline{b}}_3$ propagates back to interface 1, picking up another phase factor $e^{-j\phi/2}$ resulting in an incoming wave after one roundtrip of $\tilde{\underline{a}}_2^{(1)} = jt_1r_2e^{-j\phi}\tilde{\underline{a}}_1$. Upon reflection on interface 1, part of this wave is transmitted leading to an output

$$\tilde{\underline{b}}_1^{(1)} = jt_1jt_1r_2e^{-j\phi}\tilde{\underline{a}}_1. \tag{2.190}$$

The partial wave $\underline{a}_2^{(1)}$ is reflected again and after another roundtrip it arrives at interface 1 as $\tilde{\underline{a}}_2^{(2)} = (r_1r_2)\,e^{-j\phi}\cdot jt_1r_2e^{-j\phi}\tilde{\underline{a}}_1$. Part of this wave is transmitted and part of it is reflected back to go through another cycle. Thus in total if we sum up all partial waves that contribute to the output at port 1 of the Fabry-Perot filter, we obtain

$$\begin{aligned}
\tilde{\underline{b}}_1 &= \sum_{n=0}^{\infty}\tilde{\underline{b}}_1^{(n)} \\
&= \left(r_1 - t_1^2r_2e^{-j\phi}\sum_{n=0}^{\infty}r_1r_2e^{-j\phi}\right)\tilde{\underline{a}}_1 \\
&= \left(r_1 - t_1^2r_2\frac{e^{-j\phi}}{1-r_1r_2e^{-j\phi}}\right)\tilde{\underline{a}}_1 \\
&= \frac{r_1 - r_2e^{-j\phi}}{1-r_1r_2e^{-j\phi}}\tilde{\underline{a}}_1
\end{aligned} \tag{2.191}$$

Note, that the coefficient in front of Eq.(2.191) is the coefficient S_{11} of the scattering matrix of the Fabry-Perot. In a similar manner, we obtain

$$\begin{pmatrix} \tilde{\underline{b}}_3 \\ \tilde{\underline{b}}_4 \end{pmatrix} = \underline{\mathbf{S}}\begin{pmatrix} \tilde{\underline{a}}_1 \\ \tilde{\underline{a}}_2 \end{pmatrix} \tag{2.192}$$

and

$$\underline{\mathbf{S}} = \frac{1}{1-r_1r_2e^{-j\phi}}\begin{pmatrix} r_1 - r_2e^{-j\phi} & -t_1t_2e^{-j\phi/2} \\ -t_1t_2e^{-j\phi/2} & r_2 - r_1e^{-j\phi} \end{pmatrix} \tag{2.193}$$

In the following, we want to analyze the properties of the Fabry-Perot for the case of symmetric reflectors, i.e. $r_1 = r_2$ and $t_1 = t_2$. Then we obtain for

the power transmission coefficient of the Fabry-Perot, $|S_{21}|^2$ in terms of the power reflectivity of the interfaces $R = r^2$

$$|S_{21}|^2 = \left| \frac{1-R}{1-Re^{-j\phi}} \right|^2 = \frac{(1-R)^2}{(1-R)^2 + 4R\sin^2(\phi/2)} \tag{2.194}$$

Figure 2.50 shows the transmission $|S_{21}|^2$ of the Fabry-Perot interferometer for equal reflectivities $|r_1|^2 = |r_2|^2 = R$.

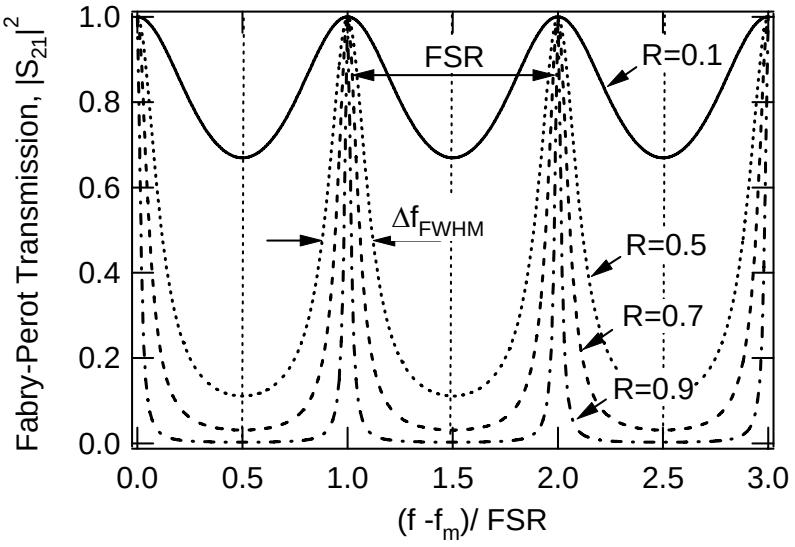

Figure 2.50: Transmission of a lossless Fabry-Perot interferometer with $|r_1|^2 = |r_2|^2 = R$

At very low reflectivity R of the mirror the transmission is almost everywhere 1, there is only a slight sinusoidal modulation due to the first order interferences which are periodically in phase and out of phase, leading to 100% transmission or small reflection. For large reflectivity R, due to the then multiple interference operation of the Fabry-Perot Interferometer, very narrow transmission resonances emerge at frequencies, where the roundtrip phase in the resonator is equal to a multiple of 2π

$$\phi = \frac{2\pi f}{c_0} n_2 2L = 2\pi m, \tag{2.195}$$

which occurs at a comb of frequencies, see Figure 2.51

$$f_m = m\frac{c_0}{2n_2L}. \tag{2.196}$$

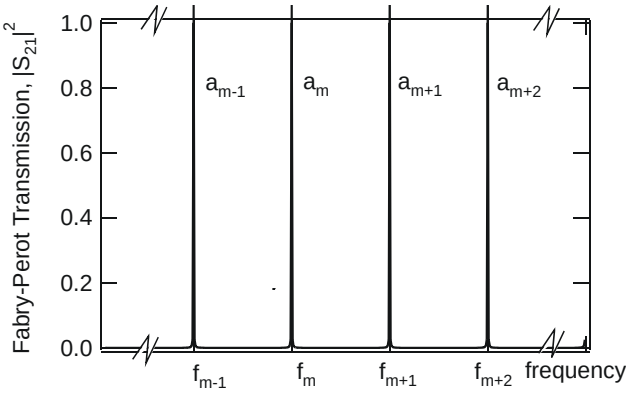

Figure 2.51: Developement of a set of discrete resonances in a one-dimensionsal resonator.

On a large frequency scale, a set of discrete frequencies, resonances or modes arise. The frequency range between resonances is called free spectral range (FSR) of the Fabry-Perot Interferometer

$$FSR = \frac{c_0}{2n_2L} = \frac{1}{T_R}, \tag{2.197}$$

which is the inverse roundtrip time T_R of the light in the one-dimensonal cavity or resonator formed by the mirrors. The filter characteristic of each resonance can be approximately described by a Lorentzian line derived from Eq.(2.194) by substituting $f = f_m + \Delta f$ with $\Delta f \ll FSR$,

$$\begin{aligned} |S_{21}|^2 &= \frac{(1-R)^2}{(1-R)^2 + 4R\sin^2\left(\left[m2\pi + 2\pi\frac{\Delta f}{FSR}\right]/2\right)} \\ &\approx \frac{1}{1+\left(\frac{2\pi\sqrt{R}}{1-R}\frac{\Delta f}{FSR}\right)^2}, \qquad (2.198) \\ &\approx \frac{1}{1+\left(\frac{\Delta f}{\Delta f_{FWHM/2}}\right)^2}, \qquad (2.199) \end{aligned}$$

where we introduced the FWHM of the transmission filter

$$\Delta f_{FWHM} = \frac{FSR}{F}, \tag{2.200}$$

with the finesse of the interferometer defined as

$$F = \frac{\pi\sqrt{R}}{1-R} \approx \frac{\pi}{T}. \tag{2.201}$$

The last simplification is valid for a highly reflecting mirror $R \approx 1$ and T is the mirror transmission. From this relation it is immediately clear that the finesse has the additional physical meaning of the optical power enhancement inside the Fabry-Perot at resonance besides the factor of π, since the power inside the cavity must be larger by $1/T$, if the transmission through the Fabry-Perot is unity.

2.3.8 Quality Factor of Fabry-Perot Resonances

Another quantity often used to characterize a resonator or a resonance is its quality factor Q, which is defined as the ratio between the resonance frequency and the decay rate for the energy stored in the resonator, which is also often called inverse photon lifetime, τ_{ph}^{-1}

$$Q = \tau_{ph} f_m. \tag{2.202}$$

Lets assume, energy is stored in one of the resonator modes which occupies a range of frequencies $[f_m - FSR/2, f_m + FSR/2]$ as indicated in Figure 2.52. Then the fourier integral

$$\underline{a}_m(t) = \int_{-FSR/2}^{+FSR/2} \underline{\tilde{b}}_2(f) e^{j2\pi(f-f_m)t}\, df, \tag{2.203}$$

where $\left|\underline{\tilde{b}}_2(f)\right|^2$ is normalized such that it describes the power spectral density of the forward traveling wave in the resonator gives the mode amplitude of the m-th mode and its magnitude square is the energy stored in the mode. Note, that we could have taken any of the internal waves $\underline{\tilde{a}}_2, \underline{\tilde{b}}_2, \underline{\tilde{a}}_3$, and $\underline{\tilde{b}}_3$. The time dependent field we create corresponds to the field of the forward or backward traveling wave at the corresponding reference plane in the resonator.

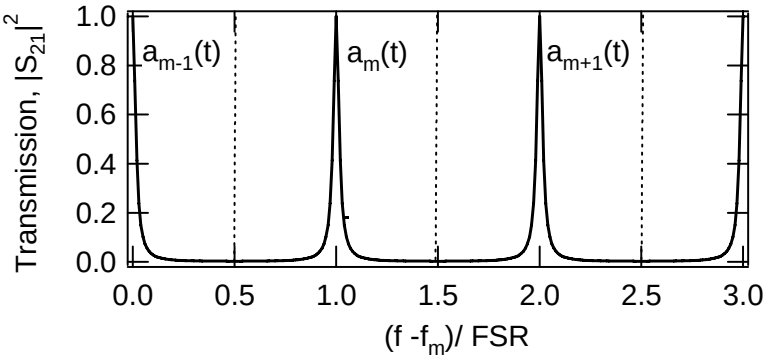

Figure 2.52: Integration over all frequency components within the frequency range $[f_m - FSR/2, f_m + FSR/2]$ defines a mode amplitude $a(t)$ with a slow time dependence

We now make a "Gedanken-Experiment". We switch on the incoming waves $\tilde{\underline{a}}_1(\omega)$ and $\tilde{\underline{a}}_4(\omega)$ to load the cavity with energy and evaluate the internal wave $\tilde{\underline{b}}_2(\omega)$. Instead of summing up all the multiple reflections like we did in constructing the scattering matrix (2.192), we exploit our skills in analyzing feedback systems, which the Fabry-Perot filter is. The scattering equations set force by the two scattering matrices characterizing the resonator mirrors in the Fabry-Perot can be visuallized by the signal flow diagram in Figure 2.53

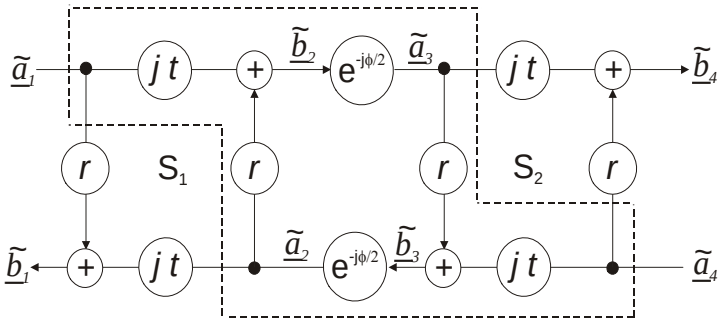

Figure 2.53: Representation of Fabry-Perot resonator by a signal flow diagram

For the task to find the relationship between the internal waves feed by the incoming wave only the dashed part of the signal flow is important. The internal feedback loop can be clearly recognized with a closed loop transfer function

$$r^2 e^{-j\phi},$$

which leads to the resonance denominator

$$1 - r^2 e^{-j\phi}$$

in every element of the Fabry-Perot scattering matrix (2.192). Using Blacks formula from 6.003 and the superposition principle we immediately find for the internal wave

$$\tilde{\underline{b}}_2 = \frac{jt}{1 - r^2 e^{-j\phi}} \left(\tilde{\underline{a}}_1 + r e^{-j\phi/2} \tilde{\underline{a}}_4 \right). \tag{2.204}$$

Close to one of the resonance frequencies, $\Omega = 2\pi f_m + \omega$, using $t = 1 - r^2$, (2.204) can be approximated by

$$\begin{aligned} \tilde{\underline{b}}_2(\omega) &\approx \frac{j}{1 + j\frac{R}{1-R}\omega T_R} \left(\tilde{\underline{a}}_1(\omega) + r(-1)^m e^{-j\omega T_R/2} \tilde{\underline{a}}_4(\omega) \right), & (2.205) \\ &\approx \frac{j}{1 + j\omega T_R/T} \left(\tilde{\underline{a}}_1(\omega) + r(-1)^m e^{-j\omega T_R/2} \tilde{\underline{a}}_4(\omega) \right) & (2.206) \end{aligned}$$

for high reflectivity R. Multiplication of this equation with the resonant denominator

$$(1 + j\omega T_R/T)\, \tilde{\underline{b}}_2(\omega) \approx j \left(\tilde{\underline{a}}_1(\omega) + r(-1)^m e^{-j\omega T_R/2} \tilde{\underline{a}}_4(\omega) \right) \tag{2.207}$$

and inverse Fourier-Transform in the time domain, while recognizing that the internal fields vanish far off resonance, i.e.

$$\underline{a}_m(t) = \int_{-\pi \cdot FSR}^{+\pi \cdot FSR} \tilde{\underline{b}}_2(\omega) e^{j\omega t}\, d\omega = \int_{-\infty}^{+\infty} \tilde{\underline{b}}_2(\omega) e^{j\omega t}\, d\omega, \tag{2.208}$$

we obtain the following differential equation for the mode amplitude slowly varying in time

$$T_R \frac{d}{dt} \underline{a}_m(t) = -T \left(\underline{a}_m(t) + j\underline{a}_1(t) + j(-1)^m \underline{a}_4(t - T_R/2) \right) \tag{2.209}$$

with the input fields

$$\underline{a}_{1/4}(t) = \int_{-\pi \cdot FSR}^{+\pi \cdot FSR} \tilde{\underline{a}}_{1/4}(\omega) e^{j\omega t}\, d\omega. \tag{2.210}$$

Despite the pain to derive this equation the physical interpretation is remarkably simple and far reaching as we will see when we apply this equation later on to many different situations. Lets assume, we switch off the loading of the cavity at some point, i.e. $\underline{a}_{1/4}(t) = 0$, then Eq.(2.209) results in

$$\underline{a}_m(t) = \underline{a}_m(0) e^{-t/(T_R/T)} \tag{2.211}$$

And the power decays accordingly

$$|\underline{a}_m(t)|^2 = |\underline{a}_m(0)|^2 e^{-t/(T_R/2T)} \tag{2.212}$$

twice as fast as the amplitude. The energy decay time of the cavity is often called the cavity energy decay time, or photon lifetime, τ_{ph}, which is here

$$\tau_{ph} = \frac{T_R}{2T}.$$

Note, the factor of two comes from the fact that each mirror of the Fabry-Perot has a transmission T per roundtrip time. For exampl a $L = 1.5m$ long cavity with mirrors of 0.5% transmission, i.e. $T_R = 10$ns and $2T = 0.01$ has a photon lifetime of 1μs. It needs hundred bounces on the mirror for a photon to be essentially lost from the cavity.

Highest quality dielectric mirrors may have a reflection loss of only $10^{-5\ldots-6}$, this is not really transmission but rather scattering loss in the mirror. Such high reflectivity mirrors may lead to the construction of cavities with photon lifetimes on the order of milliseconds.

Now, that we have an expression for the energy decay time in the cavity, we can evaluate the quality factor of the resonator

$$Q = f_m \cdot \tau_{ph} = \frac{m}{2T}. \tag{2.213}$$

Again for a resonator with the same parameters as before and at optical frequencies of 300THz corresponding to 1μm wavelength, we obtain $Q = 2 \cdot 10^8$.

2.3.9 Thin-Film Filters

Transfer matrix formlism is an efficient method to analyze the reflection and transmission properties of layered dielectric media, such as the one shown in Figure 2.54. Using the transfer matrix method, it is an easy task to compute the transmission and reflection coefficients of a structure composed of layers with arbitrary indices and thicknesses. A prominent example of a thin-film filter are Bragg mirrors. These are made of a periodic arrangement of two layers with low and high index n_1 and n_2, respectively. For maximum reflection bandwidth, the layer thicknesses are chosen to be quarter wave for the wavelength maximum reflection occures, $n_1 d_1 = \lambda_0/4$ and $n_2 d_2 = \lambda_0/4$

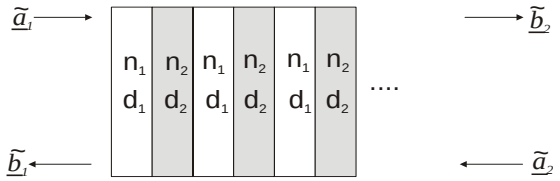

Figure 2.54: Thin-Film dielectric mirror composed of alternating high and low index layers.

As an example Figure 2.55 shows the reflection from a Bragg mirror with $n_1 = 1.45, n_2 = 2.4$ for a center wavelength of $\lambda_0 = 800$nm. The layer thicknesses are then $d_1 = 134$nm and $d_2 = 83$nm.

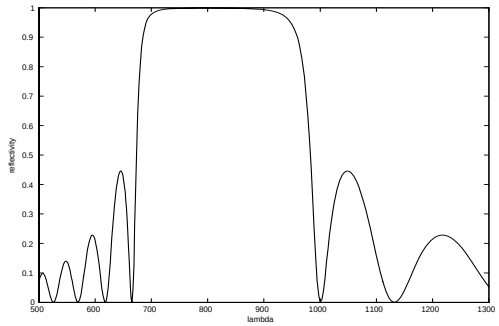

Figure 2.55: Reflectivity of an 8 pair quarter wave Bragg mirror with $n_1 = 1.45$ and $n_2 = 2.4$ designed for a center wavelength of 800nm. The mirror is embedded in the same low index material.

2.4 Paraxial Wave Equation and Gaussian Beams

So far, we have only treated optical systems operating with plane waves, which is an idealization. In reality plane waves are impossible to generate because of there infinite amount of energy required to do so. The simplest (approximate) solution of Maxwell's equations describing a beam of finite size is the Gaussian beam. In fact many optical systems are based on Gaussian beams. Most lasers are designed to generate a Gaussian beam as output. Gaussian beams stay Gaussian beams when propagating in free space. However, due to its finite size, diffraction changes the size of the beam and lenses are imployed to reimage and change the cross section of the beam. In this section, we want to study the properties of Gaussian beams and its propagation and modification in optical systems.

2.4.1 Paraxial Wave Equation

We start from the Helmholtz Equation (2.18)

$$\left(\Delta + k_0^2\right) \widetilde{\vec{E}}(x,y,z,\omega) = 0, \tag{2.214}$$

with the free space wavenumber $k_0 = \omega/c_0$. This equation can easily be solved in the Fourier domain, and one set of solutions are of course the plane waves with wave vector $|\vec{k}|^2 = k_0^2$. We look for solutions which are polarized in x-direction

$$\widetilde{\vec{E}}(x,y,z,\omega) = \widetilde{E}(x,y,z)\ \vec{e}_x. \tag{2.215}$$

We want to construct a beam with finite transverse extent into the x-y-plane and which is mainly propagating into the positive z-direction. As such we may try a superposition of plane waves with a dominant z-component of the k-vector, see Figure 2.56. The k-vectors can be written as

$$\begin{aligned} k_z &= \sqrt{k_0^2 - k_x^2 - k_y^2}, \\ &\approx k_0 \left(1 - \frac{k_x^2 - k_y^2}{2k_0^2}\right). \end{aligned} \tag{2.216}$$

with $k_x, k_y << k_0$.

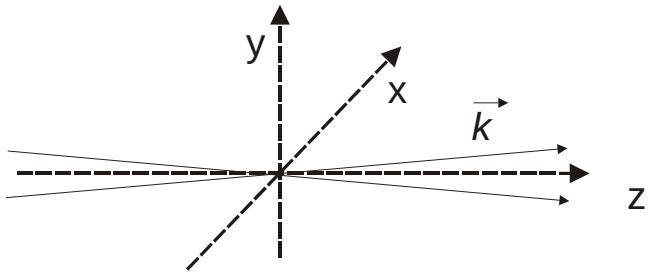

Figure 2.56: Construction of a paraxial beam by superimposing many plane waves with a dominante k-component in z-direction.

Then we obtain for the propagating field

$$\begin{aligned}\widetilde{E}(x,y,z) &= \int_{-\infty}^{+\infty}\int_{-\infty}^{+\infty}\widetilde{E}_0(k_x,k_y)\cdot \\ &\quad \exp\left[-jk_0\left(1-\frac{k_x^2+k_y^2}{2k_0^2}\right)z - jk_x x - jk_y y\right]dk_x dk_y, \\ &= \int_{-\infty}^{+\infty}\int_{-\infty}^{+\infty}\widetilde{E}_0(k_x,k_y)\cdot \\ &\quad \exp\left[j\left(\frac{k_x^2+k_y^2}{2k_0}\right)z - jk_x x - jk_y y\right]dk_x dk_y e^{-jk_0 z}, \quad (2.217)\end{aligned}$$

where $\widetilde{E}_0(k_x,k_y)$ is the amplitude for the waves with the corresponding transverse k-component. This function should only be nonzero within a small range $k_x, k_y \ll k_0$. The function

$$\widetilde{E}_0(x,y,z) = \int_{-\infty}^{+\infty}\int_{-\infty}^{+\infty}\widetilde{E}_0(k_x,k_y)\exp\left[j\left(\frac{k_x^2+k_y^2}{2k_0}\right)z - jk_x x - jk_y y\right]dk_x dk_y \quad (2.218)$$

is a slowly varying function in the transverse directions x and y, and it can be easily verified that it fulfills the paraxial wave equation

$$\frac{\partial}{\partial z}\widetilde{E}_0(x,y,z) = \frac{-j}{2k_0}\left(\frac{\partial^2}{\partial x^2}+\frac{\partial^2}{\partial x^2}\right)\widetilde{E}_0(x,y,z). \quad (2.219)$$

Note, that this equation is in its structure identical to the dispersive spreading of an optical pulse. The difference is that this spreading occurs now in the two transverse dimensions and is called diffraction.